Mechanisms Governing Longitudinal AC Breakdown at Solid-Solid Interfaces

Emre Kantar[†§]
[†]Department of Electric Power Engineering, Norwegian University of Science and Technology, Trondheim, Norway
[§]Department of Electric Power Technology, SINTEF Energy Research, Trondheim, Norway

***Abstract*—Insulation systems incorporating multilayer dielectrics are commonly used in many high-voltage applications where the interfaces between the dielectric layers are the most vulnerable regions. The primary purpose of this paper is to elucidate the mechanisms theoretically and experimentally that govern the AC breakdown of solid-solid interfaces. Two different polymers with different elastic moduli were tested. The interfaces were formed between the same specimens and were AC breakdown tested at various contact pressures. In addition, interface surfaces were polished using two different sandpapers of different grit sizes to study the effect of surface roughness. A comprehensive interface breakdown model was employed to scrutinize morphologies of solid-solid interfaces in relation to the measured interfacial AC breakdown and PD inception field strengths. PD activity in the cavities and electrical tracking resistance of contact spots between the cavities were found to be significantly affecting the interfacial breakdown phenomenon.**

I. Introduction

Dielectric strength of solid insulation materials ultimately determines the long-term electrical properties of the complete insulation system. When two nominally flat surfaces make contact, the actual surface is not perfectly smooth, and the actual contact at the interface is also not ideal, leading to numerous microcavities between adjacent contact spots. The interfacial breakdown between two solid dielectric surfaces has been reported to represent one of the principal causes of failure for insulation systems [1]; thus, a better understanding of the mechanisms governing the solid-solid interface breakdown is vital. Cavities may cause partial discharges (PD) and trigger interfacial tracking that can eventually lead to a premature electrical breakdown (BD) [2], [3]. An interface, thus, is a weak point likely to reduce the tangential AC breakdown strength (BDS) of a high-voltage (HV) insulation system due to local electric field enhancements in the cavities [2]–[5].

Scholars have mainly investigated the characteristics of insulation materials, such as the bulk BDS, surface flashover, surface tracking, and erosion without investigating the solid-solid interfaces separately [6]. Few studies have focused on the interfacial HV insulation performance between two solid dielectrics [2]–[4]. It was reported that the elasticity and surface roughness of solid materials, dielectric medium surrounding the interfaces, and contact pressure (interfacial pressure) are important factors, affecting the dielectric strength of an interface. Besides, the author's previous studies [5], [7]–[9] demonstrated significant dependency of the tangential AC BDS of solid interfaces on these factors. However, neither the mechanisms governing the interfacial BD nor the correlation between the shape/size, number of cavities (size of contact area) and the interfacial BD has yet been fully understood. Therefore, the main objective of this work is to examine the main mechanisms that control/affect the electrical BDS of interfaces between solid insulating components.

Individual effects of the contact pressure, surface roughness, and elastic modulus on the longitudinal/tangential AC BDS of solid-solid interfaces were studied, both theoretically and experimentally. In the experiments, tangential AC BDS and PD inception field strength (PDIE) of solid-solid interfaces were measured under different interface pressures, roughness levels, and elasticities. The interface contact surface model developed in [10] was employed to analyze the trends observed in the experiments and discuss the possible mechanisms controlling the interfacial breakdown.

II. Modeling the Longitudinal AC Breakdown of Solid-Solid Interfaces

The shape, size, and number of cavities and contact spots strongly affect the breakdown strength of an interface. Since the dielectric strength of a gas-filled cavity is notably lower than that of bulk insulation, cavity discharge (i.e., PD activity) can be presumed to start in the cavities first [11]. Our previous studies have suggested that discharged cavities do not necessarily lead to an interface breakdown immediately. Interfacial tracking/PD resistances of the insulation materials, forming an interface, determine the endurance of the contact spots against breakdown [12]–[15]. Therefore, we hypothesized that the electrical breakdown of a solid-solid interface should incorporate not only the discharge of air-filled cavities but also the breakdown of contact spots enclosing those cavities [9].

The interface breakdown model, thus, incorporates two submodels consisting of a model for the discharge of cavities and a model for the breakdown of contact spots. The statistical model proposed in [10] was used to develop the submodel for the cavity discharge, which estimates the BDS of average-sized cavities where the average cavity size varies based upon the given elasticity, surface roughness, and contact pressure. The submodel for the breakdown of contact spots was developed using the empirical model presented in [9], based on the interfacial tracking resistance of solid materials where enhanced field strengths at the edges of discharged cavities were approximated by a needle-needle electrode configuration.

This is the accepted version of an article published in 2020 IEEE Conference on Electrical Insulation and Dielectric Phenomena - CEIDP
http://dx.doi.org/10.1109/CEIDP49254.2020.9437443

Cavities and contact spots connected in series comprise the electrical breakdown model of an interface along which the applied voltage is distributed, as illustrated in Fig. 1:

$$V_{app} = \sum_{j=1}^{n} V_{cav_j} + \sum_{j=1}^{n} V_{cnt_j}, \quad (1)$$

where V_{app} is the applied voltage across the dry interface, n is the number of cavity and contact spot pairs, V_{cav_j} is the voltage drop across the j^{th} cavity, and V_{cnt_j} is the voltage drop across j^{th} contact spot located between two cavities, as presented in Fig. 1. Note that the contact spots in the model stand for ideal void-free contact areas.

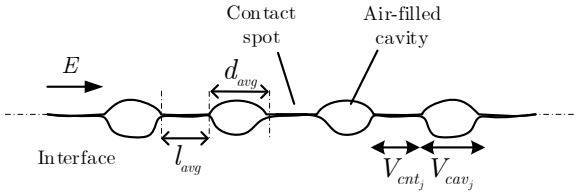

Fig. 1: Illustration of an interface consisting of cavities and contact spots. Voltage drops at the cavities and contact spots are illustrated where E is the electric field strength at the interface in the longitudinal direction.

The time frame of an interfacial breakdown, from no discharge activity to a complete flashover, is dissected in four consecutive periods. Therefore, cavity discharge and breakdown of contact spots will be initiated at different instants in a sequence. The activation order of these mechanisms is explained using the illustration shown in Fig. 2:

1) *No PD*: This is the period from the application of AC voltage until the *instant I* in Fig. 2. The electric field is not sufficiently strong to accelerate a free electron to start an avalanche mechanism in the cavities or absence of free electrons cause the delay of PD inception. Thus, no PD activity is observed in this period.

2) *Onset of PDs*: At the *instant I*, the electric field is sufficiently high to initiate a persistent discharge activity in the cavities. However, the breakdown of contact spots does not occur as yet, because the interfacial tracking resistance of the contact spots can withstand the locally enhanced fields. Thus, only PD occurs in all the average-sized cavities (Fig. 2) based on the simplified model in Fig. 1.

3) *Initiation and propagation of the interfacial tracking*: It is represented by the *instant II*. As mentioned in [9], the submodel for the interfacial tracking mechanism is operative at higher local electric fields with a BD time of around 10^{-7} s [13]. Therefore, it takes only a fraction of a microsecond from the inception of an interfacial tracking to a breakdown of the contact spots between two discharged cavities.

4) *Breakdown of the interface*: The electrodes are bridged, and the destructive effects of the interfacial breakdown are clear at the material surfaces (as revealed in Fig. 5).

III. Experimental Procedure

To test the tangential AC BDS of solid-solid interfaces as a function of elasticity, we employed two different interfaces using two different polymers with different elastic moduli. The

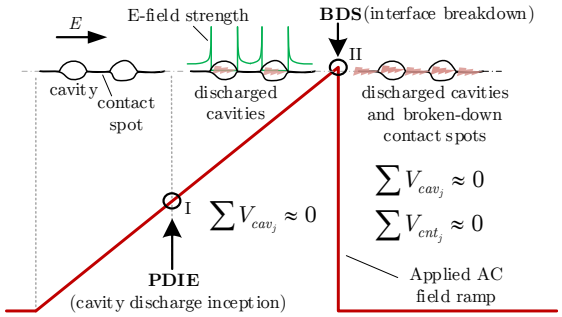

Fig. 2: Activation sequence of the mechanisms with respect to the applied AC ramp voltage. Roman numerals, I and II stand for *instant I* and *instant II*, as referred to in the text.

interfaces were assembled at dry conditions between the same materials: cross-linked polyethylene (XLPE) and polyether ether ketone (PEEK) under various contact pressures (i.e., XLPE–XLPE and PEEK–PEEK). Desired contact pressure was exerted using weights varying between 10–75 kg (0.5–3.34 MPa) to press the samples vertically against one another. The relative permittivities of XLPE and PEEK are 2.3 and 2.8, respectively. The materials were cut/prepared in rectangular prism-shaped samples (4 mm × 55 mm × 30 mm), and two samples were positioned vertically on top of each other between two Rogowski-shaped electrodes (tangential interface length: 4 mm). The contact surfaces of the samples were polished using a table-top, grinding machine. We fixed the specimens in a steel rotating disk and positioned a round-SiC sandpaper on the rotating plate [8]. To study the effect of surface roughness on the tangential AC interfacial BDS and PDIE, XLPE samples of two different surface roughnesses were used. Contact surfaces were polished using two different sandpapers of different grit sizes: #180 (rough) and #2400 (smooth). The surface roughnesses of the polished interfaces were quantified using a 3D-optical profilometer (Bruker ContourGT-K). For the experiments to study the effect of the material elasticity, all the XLPE and PEEK samples were polished using #500-grit sandpaper. The experimental setup (for AC breakdown and PD tests) and the experimental procedure were presented in minute detail for the interested readers in [5], [9]. A 50-Hz AC ramp voltage at the rate of 1 kV/s was applied until breakdown or PD inception, respectively.

IV. Results and Discussion

The effect of the cavity discharge and the breakdown of contact spots on the interfacial breakdown strength were examined separately based on the corresponding submodels introduced in Section II by following the sequence of mechanisms shown in Fig. 2. It should be emphasized that the mechanisms controlling the interface breakdown were investigated for samples assembled in optimal and dry laboratory conditions (dry-mate).

Firstly, estimated PDIE values (using the model proposed in [9], [10]) were associated with the experimentally obtained PDIE and BDS values. Next, the enhanced field E_{enh} values were calculated separately at the *instants I* and *II* (using the point-point electrode approximation proposed in [9]). The estimated enhanced fields were then compared to the estimated PD resistance E_{tr} of the insulation (using the empirical model

This is the accepted version of an article published in 2020 IEEE Conference on Electrical Insulation and Dielectric Phenomena - CEIDP
http://dx.doi.org/10.1109/CEIDP49254.2020.9437443

demonstrated in [9]) to assess whether the contact spots can endure the intense field at their edges.

A. Effect of Cavity Discharge on the Interfacial Breakdown

In this section, the correlation between the estimated cavity partial discharge field ($PDIE^e$) and the measured values (AC breakdown field and PDIE) is examined. It should be noted that the measured PDIE values do not necessarily characterize the inception field of the discharged cavities that had initiated an interfacial breakdown. Based on the 3D interface simulation results reported in [16], interfacial tracking is likely to be tortuous due to the presence of contact spots obstructing the propagation of streamers. The endurance of the contact spots against propagating streamers is designated using the interfacial tracking resistance of the contact spots (as introduced in Section II), which is an insulation property of the bulk material. Moreover, cavity sizes are essential for the theoretical analysis of the interface breakdown phenomenon. However, sizes of the interfacial cavities cannot be extracted from the measured PDIE (i.e., $PDIE^m$) data without using an analytical model. For these reasons, the statistical interface model proposed in [9], [10] was employed to determine the average sizes of cavities as a function of the surface roughness, elasticity, and applied contact pressure. The estimated average sizes of the cavities were then used to estimate the cavity discharge inception field (i.e., $PDIE^e$), as described in [10].

To begin with, the results of the AC breakdown experiments were compared to the measured PDIE values ($PDIE^m$). Fig. 3(a) shows the comparison between the measured PDIE and the measured AC BDS of the XLPE–XLPE #500 interface. The difference between the 63.2% BDS and $PDIE^m$ was found to be only around 10%, implying that discharged cavities in the XLPE samples triggered a complete flashover in a short time. In contrast, in the case of PEEK–PEEK #500 interface [Fig. 3(a)], the mean $PDIE^m$ values were lower than the measured mean BDS values by a factor of 1.6, suggesting that the contact spots at the PEEK interface could withstand discharges for a longer period (applied voltage was higher by 1 kV every next second). Overall, the correlation between the measured PDIE and BDS values, despite the limited number of data points, agrees with the proposed interfacial BD model that assumes that the interfacial tracking resistance is an essential electrical insulation property in the breakdown of interfaces.

Secondly, extended results are presented in Fig. 3(b), that cover more data points at a wider pressure range from the AC breakdown experiments performed using XLPE and PEEK with the same surface roughness (#500) as well as the estimated PDIE values.[1] The results shown in Fig. 3(b) suggest a strong correlation between the BDS values and the $PDIE^e$ values within the covered pressure range in the case of relatively soft interfaces, such as XLPE–XLPE #500. The ratio of the mean BDS to the mean $PDIE^e$ ranged from 0.8 to 1.2. The $\pm 20\%$ deviation suggests that the interfacial breakdown is likely to be dominated by the cavity discharge between the XLPE samples. Nevertheless, PEEK–PEEK #500 interfaces exhibited a relatively weak correlation between the cavity discharge and the interface breakdown, especially at relatively high contact pressures. It can be inferred that, at higher elastic modulus (harder interfaces), the interfacial breakdown is not solely governed by the discharge of vented air-filled cavities (channels), particularly at high contact pressures. Electrical insulation properties, such as the tracking resistance, are likely to play a vital role in determining the endurance of the contact spots against breakdown. The influence of the interfacial tracking resistance of the contact spots on the interfacial breakdown is discussed in the next section.

Thirdly, the results of the AC breakdown experiments carried out using XLPE samples with very rough (#180) and very smooth (#2400) interfacial surfaces and the corresponding estimated PDIE values, $PDIE^e$, are shown in Fig. 3(c). Experimental results indicated that the interfacial BDS reduced as the surface roughness was increased, whereas higher contact pressure led to an increased BDS. The 63.2% BDS in the case of the XLPE surface polished by #2400 was nearly twice as high as that in the case of XLPE #180 at each contact pressure. (Interested readers can refer to the extensive results incorporating intermediate roughnesses presented in [10].) These findings indicate a strong correlation between the estimated PDIE and the measured BDS in the case of relatively

[1]PD experiments were carried out only at two different contact pressures while the BD experiments were performed at four different pressures. The min./max. pressure values were determined based on initial tests [9].

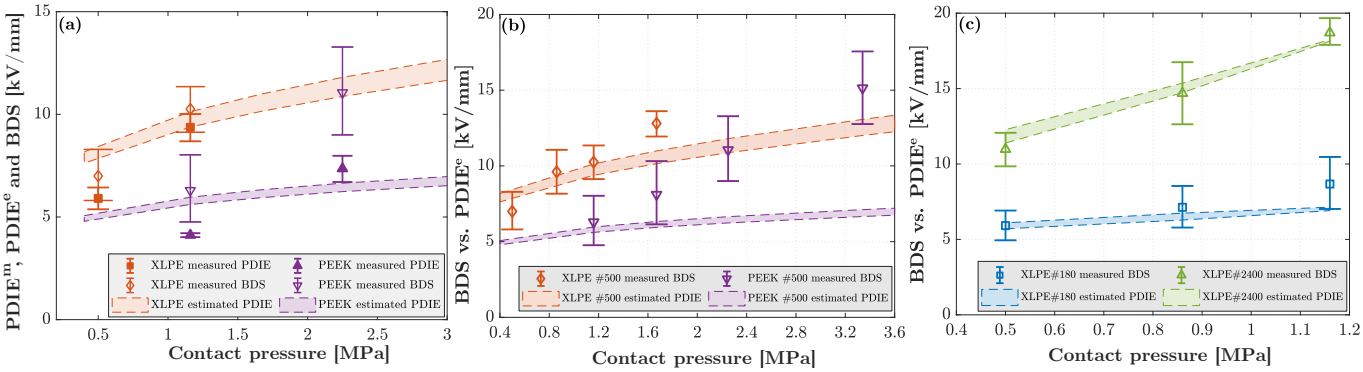

Fig. 3: Comparison of: (a) Measured PDIE ($PDIE^m$), estimated PDIE ($PDIE^e$) and measured AC BDS of XLPE–XLPE #500 and PEEK–PEEK #500 interfaces. (b) $PDIE^e$ and AC BDS of XLPE–XLPE #500 and PEEK–PEEK #500 interfaces. (c) $PDIE^e$ and AC BDS of XLPE–XLPE #180 and XLPE–XLPE #2400 interfaces.

This is the accepted version of an article published in 2020 IEEE Conference on Electrical Insulation and Dielectric Phenomena - CEIDP
http://dx.doi.org/10.1109/CEIDP49254.2020.9437443

soft interfaces such as XLPE regardless of the contact pressure. At higher contact pressures, smoother interfaces may yield a stronger correlation, as in the case of XLPE–XLPE #2400. The reader should bear in mind that the PDIE^{e} values were estimated with the assumption that all cavities are vented, and the pressure inside thereof remains at 1 atm [9], [10]. The effect of increased gas pressure inside enclosed cavities on the interfacial BDS was discussed in [16] based on 3D simulations of interfacial topographies.

B. Effect of Contact Spots on the Interfacial Breakdown

Fig. 4 compares the estimated local field enhancements at the edges of the discharged cavities E_{tr} along with the estimated PD resistances E_{tr} of XLPE, EPOXY, and PEEK (of #500 roughness for all). Tough the results of XLPE and PEEK are mainly shown in this work, the E_{tr} and E_{tr} values in the case of EPOXY is also retained to reveal how a material with an intermediate elasticity between XLPE and PEEK behaves. Based on the convention in Fig. 2, *instant I* stands for the inception of discharge in the averaged-sized cavities, whereas *instant II* represents the moment when the contact spots succumb to the intense local fields stemming from the discharged cavities and break down. Based on the method described in [9], we estimated E_{enh} and E_{tr} values using equations (5)–(6) presented in [9].

The estimated E_{enh} and E_{tr} values are displayed in Fig. 4 at both instants. Fig. 4(a) indicates that once the cavities are discharged, the low estimated tracking resistance of the XLPE is not likely to endure the enhanced local fields, and this will probably lead to an interfacial breakdown. This finding clearly supports the clear correlation between the estimated cavity discharge field and the measured interface BDS values in the case of XLPE (observed in Fig. 3): The small difference (10%) between the 63.2% BDS and PDIE^{m} values suggest that discharged cavities in XLPE probably evolved to a complete flashover in a short time because the contact spots were less likely to withstand the enhanced fields for a longer period due to the relatively low estimated interfacial tracking resistance of XLPE. Conversely, the estimated enhanced local field may not be sufficiently high to exceed the interfacial tracking resistance in the case of hard materials such as PEEK. Although the average-sized cavities were assumed to be discharged, the high estimated interfacial tracking resistance of the contact spots at the PEEK interface seems to have withstood the high local fields longer than the XLPE interface lasted. These findings are consistent with the weak correlation between the estimated PDIE and the measured interface BDS values observed in the case of PEEK–PEEK #500 in Fig. 3(b). Overall, the interfacial tracking resistance appears to have an essential role in the interfacial breakdown.

In the cases of the XLPE samples with two different surface roughnesses, when discharge activity starts in the average-sized cavities, the estimated enhanced fields are close to the estimated interfacial tracking resistance of the XLPE, as presented in Fig. 4(b). At smoother interfaces, the estimated enhanced field values appear to be sufficiently intense to

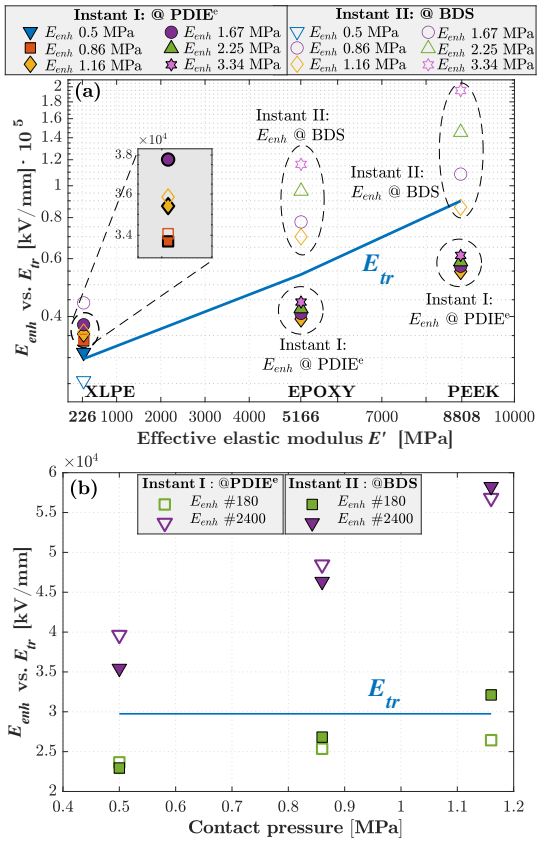

Fig. 4: Estimated enhanced fields E_{enh} vs. tracking resistance E_{tr} within the covered p_a for each interface at the instants of cavity discharge and breakdown of contact spots: (a) XLPE #500, EPOXY #500, and PEEK #500 interfaces. (b) XLPE #500 interfaces at four different surface roughnesses. Instants I and II represent the moments when PD and BD take place, respectively, in the interface BD model presented in Fig. 2.

result in a breakdown of the contact spots. The magnitudes of the estimated local fields did not significantly increase from the PD inception until interface breakdown [between *instants I* and *II* in Fig. 4(b)] because the estimated PDIE^{e} values were close to the measured BDS values. In some cases, PDIE^{m} values were estimated to be higher than the measured BDS values. Thus, the clear correlation between the cavity discharge and the interface breakdown, observed in the case of XLPE #500 in Figs. 3(a)–b, was also discerned in the case of XLPE samples with different surface roughnesses. Consequently, Fig. 4(b) highlights again that once the average-sized cavities are discharged, the low (estimated) interfacial tracking resistance of the XLPE is not likely to withstand the enhanced local fields long enough to prevent an interfacial breakdown from occurring in a short time. These findings strengthen the hypothesis that the tracking resistance of a dielectric strongly affects the interfacial breakdown as well as the discharged cavities. In particular, the results suggest that the influence of the contact spots on the interfacial BDS becomes more prominent at higher contact pressures, harder materials and/or smoother surfaces.

Interface surfaces inspected using a digital microscope after the experiments provide supporting evidence for the effect of

This is the accepted version of an article published in 2020 IEEE Conference on Electrical Insulation and Dielectric Phenomena - CEIDP
http://dx.doi.org/10.1109/CEIDP49254.2020.9437443

contact spots on the interfacial breakdown. Fig. 5(a) displays the surface of an XLPE sample that underwent an interface breakdown. The encircled area at the surface indicates interfacial microtracking activity near the top electrode, but the propagation of the streamers was most likely hindered due to the contact spots on their way. The interface tracking path shown by the arrows might be one such streamer that could propagate owing to connected cavities or by breaking down the contact spots obstructing it. The surface of a PEEK sample, subjected to an interfacial breakdown, provides more explicit evidence, as shown in Fig. 5(b). The enclosed area unveils an interfacial microtrack of a length of about 0.24 mm. The tracking path is located near the main breakdown track, but neither of its ends is connected with other tracking paths. Thus, it is an isolated microtrack, which possibly bridged two contact areas but was stopped by the high tracking resistance of the contact spots at PEEK. The images suggest that there were discharge activities in several cavities/channels that could not evolve to a complete flashover.

Last but not least, we evaluated varying the elastic modulus by adding micro- and nano-scaled fillers/particles, yet our research suggested that adding such fillers causes as significant a change in the chemical/electrical properties as does selecting a different polymer [17]. Therefore, we decided to choose materials widely-used in power cables and accessories.

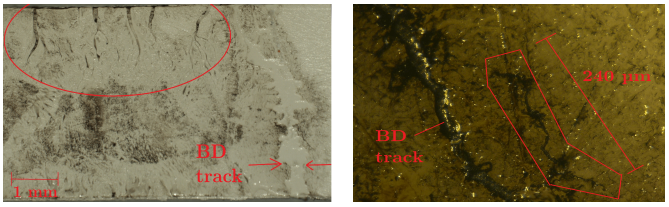

(a) XLPE–XLPE #500 1.16 MPa. (b) PEEK–PEEK #500 1.16 MPa.

Fig. 5: Microtracking observed at interfaces between broken-down samples. The widths of the microtracks range from 4–8 µm.

V. Conclusion

The results of experimental and theoretical studies performed in this work have indicated that different mechanisms are involved in the breakdown of air-filled cavities and contact spots. The main hypothesis—that size, shape and insulating medium strongly affect the discharge inception field of the cavities, whereas, the interfacial tracking resistance of the contact spots enclosing the cavities also has a significant impact on the interfacial breakdown strength—has been verified using the results of the experimental and theoretical studies.

The interfacial breakdown in the cases of softer materials such as XLPE–XLPE has been found to be strongly dominated by the discharged cavities due to the relatively low estimated interfacial tracking resistance XLPE. In other words, discharged cavities have resulted in an interfacial failure more easily because the contact spots could not withstand the enhanced fields for a long time. In addition, different surface roughnesses in the case of XLPE–XLPE interfaces have also suggested a clear correlation between the cavity discharge and the interface breakdown in the cases of rough and smooth surfaces. On the other hand, in the case of hard interfaces with higher elastic modulus such as PEEK–PEEK, contact spots may have endured the local enhanced fields longer due to the relatively high estimated tracking resistance of PEEK. To conclude, the results have suggested that the influence of the interfacial tracking resistance of contact spots on the interface breakdown becomes more prominent at higher contact pressures, interfaces between harder materials and/or smoother surfaces.

To our knowledge, the proposed theoretical model is novel in incorporating diverse interdisciplinary fields to model interface breakdown at solid-solid interfaces. As a result of the clear agreement between the theoretical results and experimental results, we believe that the model deserves further attention.

References

[1] D. Kunze, B. Parmigiani, R. Schroth, and E. Gockenbach, "Macroscopic internal interfaces in high voltage cable accessories," in *CIGRE Session*, 2000, pp. 15–203.

[2] B. Zhu, Z. Jia, H. Hu, X. Ouyang, and X. Wang, "Relationship between the Interfacial Ramped DC Breakdown Voltage and the Morphology of the XLPE/SiR Interface," *IEEE Trans. Dielectr. Electr. Insul.*, vol. 26, no. 3, pp. 689–697, Jun. 2019.

[3] B. Du, X. Zhu, L. Gu, and H. Liu, "Effect of surface smoothness on tracking mechanism in XLPE-Si-rubber interfaces," *IEEE Trans. Dielectr. Electr. Insul.*, vol. 18, no. 1, pp. 176–181, 2011.

[4] M. Kato, Y. Nishimura, N. Osawa, Y. Yoshioka, H. Yanase, and K. Okamoto, "Effects of Compressive Force and Dielectric Materials on Contact Area for High-Pressure Region and Interfacial AC Breakdown Between Two Solid Dielectrics," in *Proc. 21st Int. Symp. HV Eng. (ISH 2019)*. Springer Int., 2020, pp. 118–129.

[5] E. Kantar, "Longitudinal AC Electrical Breakdown Strength of Polymer Interfaces," Ph.D. dissertation, Norwegian Uni. Sci. Tech., 2019.

[6] D. Fournier and L. Lamarre, "Effect of pressure and length on interfacial breakdown between two dielectric surfaces," in *IEEE Int. Symp. Electr. Insul.*, 2005, pp. 270–272.

[7] E. Kantar, D. Panagiotopoulos, and E. Ildstad, "Factors Influencing the Tangential AC Breakdown Strength of Solid-Solid Interfaces," *IEEE Trans. Dielectr. Electr. Insul.*, vol. 23, no. 3, pp. 1778–1788, 2016.

[8] E. Kantar, S. Hvidsten, F. Mauseth, and E. Ildstad, "Longitudinal AC Breakdown Voltage of XLPE-XLPE Interfaces Considering Surface Roughness and Pressure," *IEEE Trans. Dielectr. Electr. Insul.*, vol. 24, no. 5, pp. 3047–3054, 2017.

[9] E. Kantar, S. Hvidsten, and E. Ildstad, "Effect of Material Elasticity on the Longitudinal AC Breakdown Strength of Solid-Solid Interfaces," *IEEE Trans. Dielectr. Electr. Insul.*, vol. 26, no. 2, pp. 655–663, 2019.

[10] E. Kantar, S. Hvidsten, F. Mauseth, and E. Ildstad, "A Stochastic Model for Contact Surfaces at Polymer Interfaces Subjected to an Electrical Field," *Tribology Int.*, vol. 127, pp. 361–371, 2018.

[11] H. Illias, G. Chen, and P. L. Lewin, "Modeling of partial discharge activity in spherical cavities within a dielectric material," *IEEE Electr. Insul. Mag.*, vol. 27, no. 1, pp. 38–45, Jan. 2011.

[12] X. Chen, Y. Xu, X. Cao, and S. M. Gubanski, "Electrical treeing behavior at high temperature in XLPE cable insulation samples," *IEEE Trans. Dielectr. Electr. Insul.*, vol. 22, no. 5, pp. 2841–2851, 2015.

[13] J. C. Fothergill, "Filamentary electromechanical breakdown," *IEEE Trans. Electr. Insul.*, vol. 26, no. 6, pp. 1124–1129, 1991.

[14] R. M. Eichhorn, "Treeing in solid extruded electrical insulation," *IEEE Trans. Electr.Insul.*, vol. EI-12, no. 1, pp. 2–18, 1977.

[15] J. H. Mason, "Assessing the resistance of polymers to electrical treeing," *IEE Proc. A: Phys. Sci. Meas. Instrum. Manage. Edu. Reviews*, vol. 128, no. 3, pp. 193–201, 1981.

[16] E. Kantar, "A Deterministic Model for Contact Surfaces at Dielectric Interfaces Subjected to an Electrical Field," in *IEEE Conf. Electr. Insul. and Dielectr. Phen. (CEIDP)*, 2020.

[17] S. Albayrak, C. Becker-Willinger, M. Aslan, and M. Veith, "Influence of nano-scaled zirconia particles on the electrical properties of polymer insulating materials," *IEEE Trans. Dielectr. Electr. Insul.*, vol. 19, no. 1, pp. 76–82, Feb. 2012.

This is the accepted version of an article published in 2020 IEEE Conference on Electrical Insulation and Dielectric Phenomena - CEIDP
http://dx.doi.org/10.1109/CEIDP49254.2020.9437443